



# Injectable biodegradable hydrogels with tunable mechanical properties for the stimulation of neurogenic differentiation of human mesenchymal stem cells in 3D culture

Li-Shan Wang, Joo Eun Chung, Peggy Pui-Yik Chan, Motoichi Kurisawa\*

*Institute of Bioengineering and Nanotechnology, 31 Biopolis Way, The Nanos, Singapore 138669, Singapore*

## ARTICLE INFO

### Article history:

Received 28 September 2009

Accepted 16 October 2009

Available online 4 November 2009

### Keywords:

Hydrogel

Neurogenesis

Human mesenchymal stem cells

Differentiation

Stiffness

## ABSTRACT

We report an injectable hydrogel scaffold system with tunable stiffness for controlling the proliferation rate and differentiation of human mesenchymal stem cells (hMSCs) in a three-dimensional (3D) context in normal growth media. The hydrogels composed of gelatin-hydroxyphenylpropionic acid (Gtn-HPA) conjugate were formed using the oxidative coupling of HPA moieties catalyzed by hydrogen peroxide ( $H_2O_2$ ) and horseradish peroxidase (HRP). The stiffness of the hydrogels was readily tuned by varying the  $H_2O_2$  concentration without changing the concentration of polymer precursor. We found that the hydrogel stiffness strongly affected the cell proliferation rates. The rate of hMSC proliferation increased with the decrease in the stiffness of the hydrogel. Also, the neurogenesis of hMSCs was controlled by the hydrogel stiffness in a 3D context without the use of any additional biochemical signal. These cells which were cultured in hydrogels with lower stiffness for 3 weeks expressed much more neuronal protein markers compared to those cultured within stiffer hydrogels for the same period of time.

© 2009 Elsevier Ltd. All rights reserved.

## 1. Introduction

Cell therapies represent a promising way to treat a variety of diseases and injuries in the area of regenerative medicine and tissue engineering [1–3]. The use of human mesenchymal stem cells (hMSCs) in cell therapies may be advantageous owing to their high accessibility and ease of handling. They have been reported to differentiate into multiple cell lineages, including osteoblasts, chondroblasts, adipocytes, neurons, skeletal myoblasts, and cardiac myocytes [4] and have played progressively prominent roles in tissue engineering due to their relative ease of isolation and no tumorigenic potential *in vivo* [5]. Recently, there has been increasing recognition that substrate mechanics [6] and the topography of the extracellular microenvironment [7] can modulate the tissue cell phenotype in a way similar to biochemical signals. When hMSCs are cultured on collagen-coated polyacrylamide gels with different stiffness, hMSCs are differentiated to neuronal, muscle, and bone cells as the stiffness of the gel is increased [8]. These results imply potential applications for hMSCs in tissue regeneration could be gained with a suitable material system that provides for the culture and differentiation of cells in a three-dimensional (3D) context, as

cells behave more physiologically in a 3D environment compared to 2D surfaces. In addition, it is essential to administer the cells to the precise location for tissue repair and regeneration [9].

The use of hydrogels as scaffolds for cultivating cells in a 3D environment is attractive, because hydrogels have high permeability for oxygen, nutrients and other water-soluble metabolites through their high water-content matrix, which is an excellent environment for cell growth and tissue regeneration [10]. Furthermore, the use of injectable hydrogels as scaffolds in tissue engineering is advantageous compared to preformed hydrogels because they are able to fill any shape or defect; they can be easily formulated with cells by simple mixing, and do not require a surgical procedure to be implanted or in the case of biodegradable ones, to be removed. Another important requirement for an injectable hydrogel system is for the hydrogel to be formed rapidly after injection, to prevent the undesirable diffusion of the gel precursors and cells to the surrounding tissues [11]. However, a major drawback of existing injectable hydrogel systems concerns the control of the gelation rate. The means of controlling the gelation rate is limited to varying the gel precursor and/or crosslinker concentration, which inevitably changes the stiffness of the hydrogel and leads to the undesirable control of the cell growth and differentiation in hydrogels. Also, such systems would require a lot of optimization in order to achieve the appropriate growth rate and control over the differentiation of cells, because different

\* Corresponding author. Tel.: +65 6824 7139; fax: +65 6478 9083.

E-mail address: [mkurisawa@ibn.a-star.edu.sg](mailto:mkurisawa@ibn.a-star.edu.sg) (M. Kurisawa).

concentrations of precursor polymer would be used to control the gelation rate. Using different concentrations of the polymer precursor may cause changes in the interaction between polymer chains and cells, especially when the polymer chains are conjugated with cell adhesive ligands such as Arg-Gly-Asp (RGD) peptides. Here, we demonstrate how this limitation can be overcome through the enzyme-mediated oxidation crosslinking reaction of gelatin-hydroxyphenylpropionic acid (Gtn-HPA) conjugates. Recently, the independent tuning of the stiffness and the gelation rate of an injectable hydrogel has been achieved by utilizing a simple solution mixture of constant concentrations of hyaluronic acid-phenol conjugates, hydrogen peroxide ( $H_2O_2$ ) and horseradish peroxidase (HRP) [12]. The hydrogels were formed through the oxidative coupling of phenol moiety, which was catalyzed by  $H_2O_2$  and HRP [12–14]. The  $H_2O_2$  and HRP determined the hydrogel stiffness and the gelation rate of the injectable hydrogel, respectively.

Neural tissue engineering is an emerging research area for the treatment of injuries of central nervous system (CNS) [15–17]. Hydrogel scaffolds have been recognized as an attractive strategy for the regeneration of damaged tissue in CNS and used to release trophic factors, bridge spinal cord defects and enhance cell infiltration [15–23]. In addition, stem cell-based tissue regeneration strategies have been widely investigated for the treatment of spinal cord and traumatic brain injuries [16]. It has been reported that 3D culture of murine embryonic and neural stem cells in hydrogel shows the enhanced neuronal differentiation [24–27]. However, it has been suggested that controlled neural differentiation of hMSCs might become an important source of cells for cell therapy of neurodegenerative diseases, since hMSCs are more easily harvested and effectively expanded than neural stem cells [28]. From these perspectives, we consider that the design of an injectable hydrogel system that differentiates hMSCs to neuronal cells would be important for the treatment of central nervous injuries. We herein report enzyme-mediated Gtn-HPA hydrogels with tunable mechanical strength for controlling cell growth and neurogenesis of hMSCs in 3D (Fig. 1).

## 2. Materials and methods

### 2.1. Materials

Gelatin (Gtn) (MW = 80–140 kDa, pI = 5) and horseradish peroxidase (HRP) (100 units/mg) were obtained from Wako Pure Chemical Industries (Japan). 3,4-

Hydroxyphenylpropionic acid (HPA), *N*-hydroxysuccinimide (NHS), 1-ethyl-3-(3-dimethylaminopropyl)-carbodiimide hydrochloride (EDC·HCl), type 1 collagenase (246 units/mg), Triton X-100, bovine serum albumin (BSA), anti- $\beta$ -tubulin, anti-neurofilament light chain (NFL) and anti-microtubule associated protein 2 (MAP2) were purchased from Sigma-Aldrich (Singapore). Anti-neurofilament heavy chain was obtained from Zymed (USA). Human mesenchymal stem cells (hMSCs) were provided by Cambrex Bio Science Walkersville, Inc. (USA). Mesencult human basal medium supplemented with mesencult human supplement was purchased from Stem Cell Technologies (Canada). Fetal bovine serum (FBS), calcein acetoxyethyl ester, 4',6-diamidino-2-phenylindole (DAPI) and fluorophore-conjugated secondary antibodies were provided by Invitrogen (Singapore). HRP-conjugated secondary antibodies were purchased from GE Healthcare (Singapore). Actin/focal adhesion stain kit were provided by Millipore (Singapore). Phosphate buffer saline (PBS, 150 mM, pH 7.3) solution was supplied by media preparation facility in Biopolis (Singapore).

### 2.2. Synthesis of Gtn-HPA conjugate

3,4-Hydroxyphenylpropionic acid (HPA) was used to synthesize Gtn-HPA conjugates by a general carbodiimide/active ester-mediated coupling reaction in distilled water [29]. HPA (3.32 g, 20 mmol) was dissolved in 250 ml of mixture of distilled water and *N,N*-dimethylformamide (DMF) (3:2). To this *N*-hydroxysuccinimide (3.20 g, 27.8 mmol) and 1-ethyl-3-(3-dimethylaminopropyl)-carbodiimide hydrochloride (3.82 g, 20 mmol) were added. The reaction was stirred at room temperature for 5 h, and the pH of the mixture was maintained at 4.7. Then, 150 ml of Gtn aqueous solution (6.25 wt.%) was added to the reaction mixture and stirred overnight at room temperature at pH 4.7. The solution was transferred to dialysis tubes with molecular cut-off of 1000 Da. The tubes were dialyzed against 100 mM sodium chloride solution for 2 days, a mixture of distilled water and ethanol (3:1) for 1 day and distilled water for 1 day, successively. The purified solution was lyophilized to obtain the Gtn-HPA.

### 2.3. Rheological measurement

Rheological measurements of the hydrogel formation were performed with a HAAKE Rheoscope 1 rheometer (Karlsruhe, Germany) using a cone and plate geometry of 35 mm diameter and 0.945° cone angle. The measurements were taken at 37 °C in the dynamic oscillatory mode with a constant deformation of 1% and frequency of 1 Hz. To avoid slippage of samples during the measurement, a roughened glass bottom plate was used. The solutions of HRP and  $H_2O_2$  with different concentrations were added sequentially to an aqueous solution of Gtn-HPA (2 wt.%, 250  $\mu$ l in PBS). The solution was vortexed and then immediately applied to the bottom plate. The upper cone was then lowered to a measurement gap of 0.024 mm and a layer of silicon oil was carefully applied around the cone to prevent solvent evaporation during the experiment. The measurement parameters were determined to be within the linear viscoelastic region in preliminary experiments.

### 2.4. Enzymatic degradation of Gtn-HPA hydrogels

For the preparation of slab-shaped Gtn-HPA hydrogels, lyophilized Gtn-HPA was dissolved in PBS at a concentration of 2 wt.%. 6  $\mu$ l of HRP was added to 1 ml of Gtn-HPA solution to give a final concentration of 0.15 units/ml. Crosslinking was

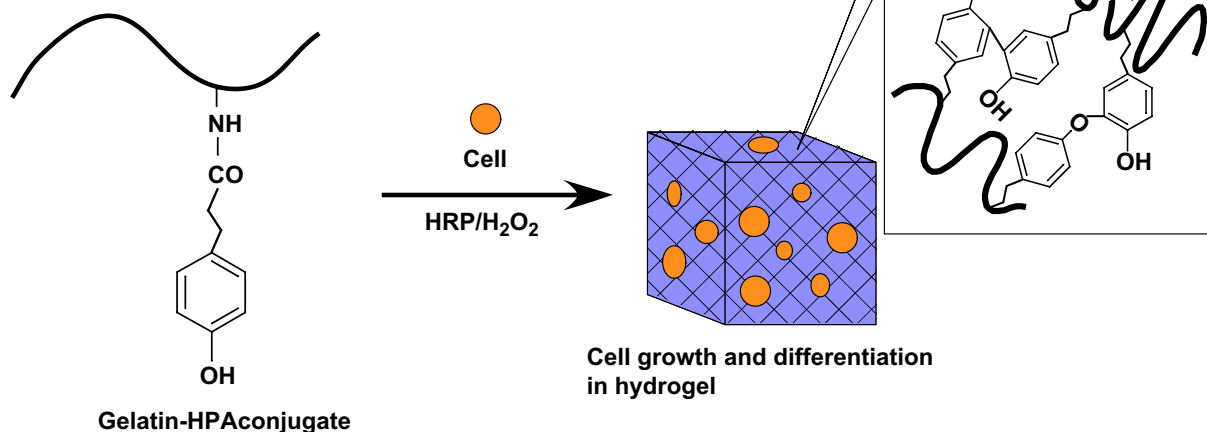


Fig. 1. *In situ* forming of Gtn-HPA hydrogel by an enzyme-catalyzed oxidation for 3D cell growth and differentiation.

initiated by adding 6  $\mu$ l of different concentrations of  $H_2O_2$  solution to give final concentrations of 0.85 and 1.7 mM. The mixture was vortexed vigorously before it was injected between two parallel glass plates clamped together with 1 mm spacing. The crosslinking reaction was allowed to proceed for 2 h. Then, round hydrogel disks with diameters of 1.6 cm were cut out from the hydrogel slab using a circular mold. The hydrogel disks were swollen in PBS for 48 h to reach swelling equilibrium and then sandwiched between plastic nets to facilitate retrieval of the hydrogels during degradation. The hydrogels were immersed in 20 ml of PBS containing 0.61 units/ml of type I collagenase and incubated at 37 °C in an orbital shaker at 100 rpm. The degree of degradation of the hydrogels was estimated by measuring the residual hydrogel weight. For measuring the residual weight, the hydrogels were removed from the solution, blotted dry and weighed at specific time points.

### 2.5. Cell attachment study

For the preparation of Gtn-HPA hydrogels in the 24-well plate, lyophilized Gtn-HPA was dissolved in PBS at a concentration of 2 wt%. 6  $\mu$ l of HRP was added to 1 ml of Gtn-HPA solution to give a final concentration of 0.15 units/ml. Crosslinking was initiated by adding 6  $\mu$ l of different concentrations of  $H_2O_2$  solution to give final concentrations of 0.85 and 1.7 mM. The hydrogels were allowed to set for 4 h. Five hundred  $\mu$ l of hMSCs in mesencult human basal medium supplemented with mesencult human supplement (passage number <6) at cell density of  $3 \times 10^5$  cells/ml were seeded onto the hydrogels. The hydrogels were incubated at 37 °C for 1 h and 6 h. After the incubation, the media with unattached cells were aspirated and the wells were washed with PBS. A culture plate without hydrogel was served as a comparison. The cells attached on the hydrogels were harvested by incubating the hydrogels with collagenase solution. The cells attached on the culture plate were harvested by trypsinization. To determine the number of attached cell on the hydrogels and culture well plate, the quantification of DNA was performed. The cell pellets were lysed by a freeze-thaw cycle in 200  $\mu$ l of DNA-free lysis buffer. Samples were then incubated with 200  $\mu$ l of PicoGreen working solution. The number of cells attached on the surfaces was then determined by the fluorescence measurement of the sample solution along with the known concentration of cell suspension for the standard curve. The fluorescence measurement was performed using a microplate reader with excitation and emission at 480 and 520 nm, respectively. This experiment was performed in four replicates.

### 2.6. Cell proliferation assay

For 2D cell proliferation on the surface of hydrogels, the hydrogels were prepared in 24-well plate using the same protocol as described above and allowed to set for 4 h. Five hundred  $\mu$ l hMSCs in mesencult human basal medium supplemented with mesencult human supplement (passage number <6) at cell density of  $2 \times 10^4$  cells/ml were seeded onto the hydrogels and maintained in culture medium. For 3D cell proliferation in the hydrogels, hMSC were mixed with 1 ml of Gtn-HPA solution (2 wt.%) in 6-well plate at final concentrations of  $1 \times 10^5$  cells/ml. To initiate gel formation, 6  $\mu$ l of  $H_2O_2$  with different concentrations and 6  $\mu$ l of HRP (25 units/ml) were added to the solution. The hydrogels were allowed to set for 4 h before being maintained in culture medium. For both 2D and 3D studies, the culture medium was changed every 2–3 days. To evaluate the cell proliferation in hydrogels, the PicoGreen assay to quantify DNA amount was performed using the same protocol as described above. For the observation of cell morphology in hydrogels, cell-encapsulated hydrogels were incubated with 2  $\mu$ M of calcein acetoxymethyl ester for 1 h at 37 °C. The morphology of fluorescently labeled cells was accessed using fluorescence microscope (Olympus 71, Japan).

### 2.7. Water uptake measurement

To monitor the change of water uptake in Gtn-HPA hydrogel over time, cell-encapsulated hydrogels were prepared as described above. Gtn-HPA hydrogels in the absence of cells were also prepared and maintained in the same culture medium as comparison. At each time interval, the hydrogels were removed from medium, blotted to remove excess aqueous medium and immediately weighed. Water uptake was calculated from the equation  $W = (M_s - M_d)/M_d$ , where  $M_s$  is the weight of the hydrogel in swollen state, and  $M_d$  is the dry weight of the hydrogel obtained by lyophilization. Three replicates were performed for this experiment.

### 2.8. Cell focal adhesion study

Both 2D and 3D cultures of hMSCs were performed using Gtn-HPA hydrogels for 2 weeks before being immunostained using an actin/focal adhesion stain kit. Prior to it, the hydrogels together with the cells were fixed with 4% formaldehyde solution at room temperature for 20 min. After washing, the cells were permeabilized using 0.5%

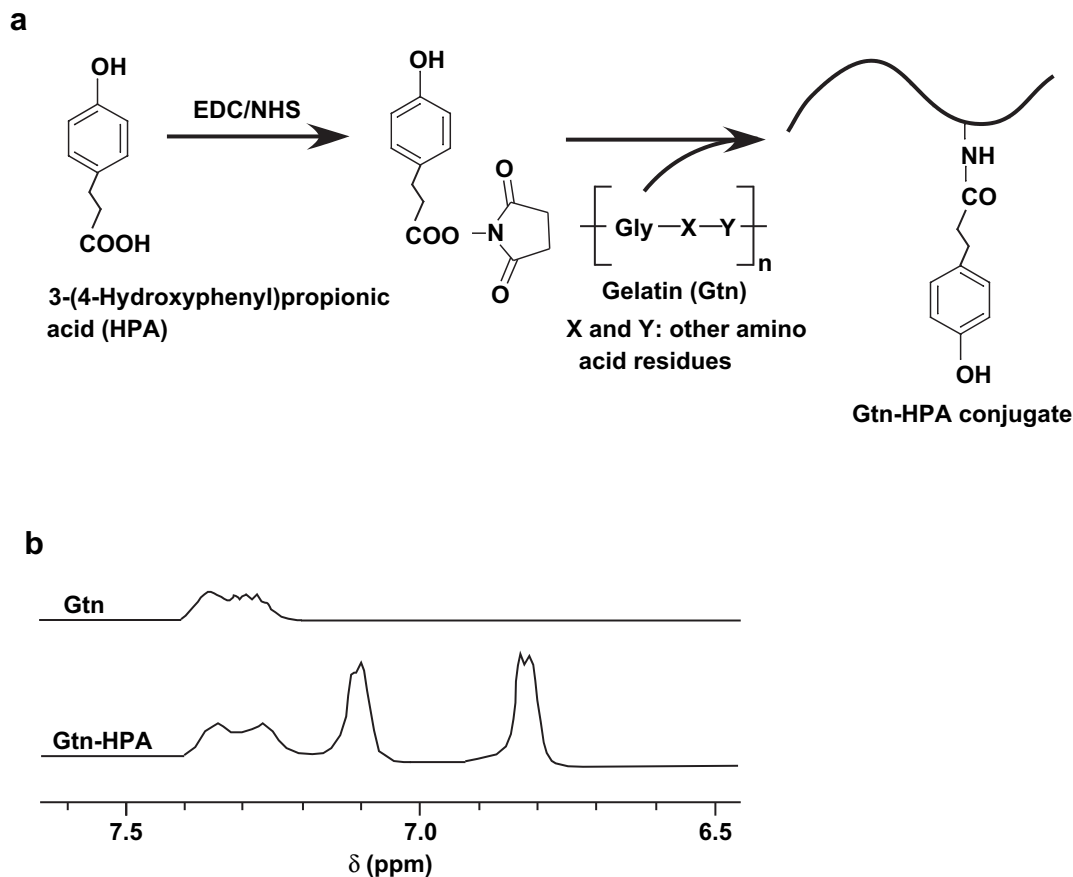


Fig. 2. Synthesis of Gtn-HPA conjugate. (a) Synthetic scheme for Gtn-HPA conjugate. (b)  $^1H$  NMR spectra of Gtn-HPA conjugate.

Triton X-100 in PBS solution at room temperature for 5 min. The cells were then blocked in 0.05% Triton X-100 containing 1% bovine serum albumin at room temperature for 1 h. The samples were then incubated with anti-vinculin in blocking buffer solution at 4 °C overnight. After washing, the cells were incubated with the FITC-conjugated secondary antibody in the dark for 30 min. For double labeling, TRITC-conjugated phalloidin was incubated simultaneously with the secondary antibody. The cell nuclei were counterstained with DAPI (1:15,000 in water of 5 mg/ml stock). Confocal images were taken with a confocal laser scanning microscopy (Olympus FV300, Japan).

### 2.9. 3D cell differentiation

For studies involving hMSC differentiation in Gtn-HPA hydrogels, the cells were pre-treated with mitomycin C (10  $\mu\text{g/ml}$ ) for 2 h to inhibit the proliferation and washed three times with culture medium. The hydrogels containing mitomycin C treated hMSCs at final density of  $1 \times 10^5$  cells/ml were prepared as described above. The culture was maintained for 3 weeks. Prior to confocal imaging, the cells were fixed, permeabilized and blocked using the same protocol as described above. The samples were then incubated with the primary antibody in blocking buffer solution at 4 °C overnight. After washing, the cells were incubated with the fluorophore-conjugated secondary antibodies in the dark for 30 min. The cell nuclei were counterstained with DAPI (1:15,000 in water of 5 mg/ml stock). Confocal images were taken with confocal laser scanning microscopy (Olympus FV300, Japan). For western blotting, cells were harvested using collagenase as described above. The cells in buffer (4% SDS, 20% glycerol and 0.02% bromophenol blue in Tris-HCl (0.125 M, pH 6.8)) were sonicated for 30 seconds. Cell lysate was boiled for 5 min, and was subjected to SDS-polyacrylamide gel electrophoresis. Proteins were transferred onto nitrocellulose, blocked, and labeled with HRP-conjugated secondary antibodies. Blot

for  $\beta$ -actin was served as a control to ensure constant protein loading level. All western blottings were performed in duplicate.

## 3. Results and discussion

### 3.1. Synthesis of Gtn-HPA conjugates

Gtn-HPA conjugates were successfully synthesized by a general carbodiimide/active ester-mediated coupling reaction in distilled water (Fig. 2a). The percentage of HPA introduced to the amine groups of Gtn was determined by the conventional 2,4,6-trinitrobenzene sulfonic acid (TNBS) method [30]. The result showed 90% of the amine group in Gtn was conjugated with HPA. The success of this conjugation was further confirmed by  $^1\text{H}$  NMR measurement. From the  $^1\text{H}$  NMR spectrum of Gtn-HPA, the peaks at chemical shift ( $\delta$ ) 6.8 ppm and 7.1 ppm indicate the presence of the aromatic protons of HPA, in addition to the aromatic protons of phenylalanine and tyrosine residues of Gtn ( $\delta = 7.3$  ppm) (Fig. 2b).

### 3.2. Hydrogel formation

A variety of chemo-induced gelation strategies including the use of glutaraldehyde and carbodiimides have been reported [31]. These

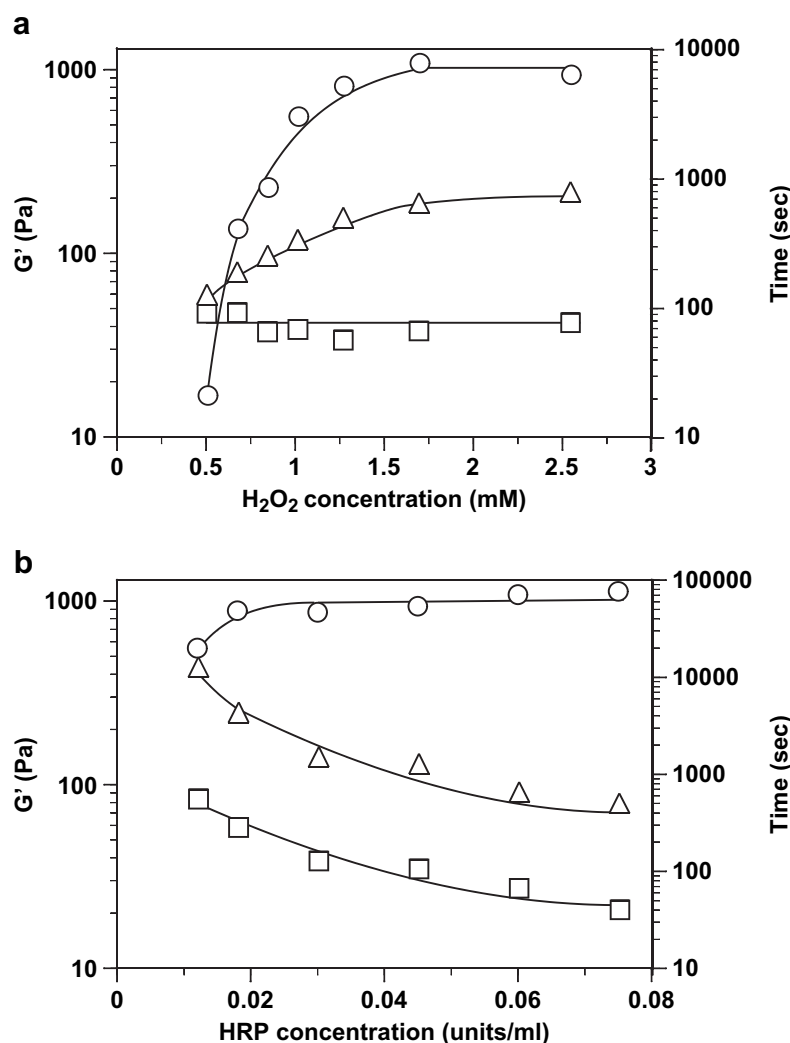


**Fig. 3.** Effects of (a)  $\text{H}_2\text{O}_2$  and (b) HRP concentration on the storage modulus  $G'$  (○), the gel point (□) and the time needed for  $G'$  to reach plateau (△). HRP and  $\text{H}_2\text{O}_2$  concentrations are fixed at 0.06 units/ml for (a) and 1.7 mM for (b) respectively.

**Table 1**  
Rheological properties of Gtn-HPA hydrogels used in the cell proliferation and differentiation study.<sup>a</sup>

Sample	Gtn-HPA (wt.%)	HRP (units/ml)	H <sub>2</sub> O <sub>2</sub> (mM)	G' (Pa)	Gel point (sec) <sup>b</sup>	Time needed for G' to reach plateau (sec)
Gtn-HPA-soft	2	0.15	0.85	281 ± 19 <sup>c</sup>	<30	78 ± 12
Gtn-HPA-stiff	2	0.15	1.7	841 ± 45	45 ± 5	251 ± 29

<sup>a</sup> Measurement was taken with constant deformation of 1% at 1 Hz and 37 °C ( $n = 4$ ). Results are shown as the average values ± standard deviation.

<sup>b</sup> Gel point is defined as the time at which the crossover of storage modulus ( $G'$ ) and loss modulus ( $G''$ ) occurred. Herein, it is used as an indicator of the rate of gelation.

<sup>c</sup> Means that the stiffness of Gtn-HPA-soft was significantly lower than that of Gtn-HPA-stiff. Differences between the values were assessed using Student's unpaired  $t$ -test and  $p < 0.05$  was considered statistically significant.

chemical modification strategies are difficult to apply to *in situ* gelation *in vivo* due to the toxicity of the cross-linking agents [32]. In this study, the Gtn-HPA hydrogel was formed using the oxidative coupling of HPA moieties catalyzed by H<sub>2</sub>O<sub>2</sub> and HRP (Fig. 1). It is well known that phenols crosslink through either a more common C–C linkage between the *ortho*-carbons of the aromatic ring or a C–O linkage between the *ortho*-carbon and the phenolic oxygen [33].

The formation of Gtn-HPA hydrogels was studied using oscillatory rheometry which measures the storage modulus ( $G'$ ) and loss modulus ( $G''$ ) against the shear strain. Rheological method has been often employed to study the viscoelastic behavior of materials and  $G'$  is commonly served an indication of stiffness of a given viscoelastic material. Also, the gel point, defined as the crossover of  $G'$  and  $G''$ , is employed to evaluate the gelation rate of hydrogel. In this study, value of  $G'$  was recorded when it reached a plateau, which indicated that crosslinking had been completed.

Fig. 3a shows the effects of H<sub>2</sub>O<sub>2</sub> concentration on the gel point, the time required for  $G'$  to reach plateau and the  $G'$  value when HRP concentration was kept at 0.06 units/ml. It was found that  $G'$  which ranged from 10 to 1000 Pa was tunable by H<sub>2</sub>O<sub>2</sub> concentration when an aqueous solution of Gtn-HPA conjugate (2 wt.%) was utilized.  $G'$  increased with the increase of H<sub>2</sub>O<sub>2</sub> concentration from 0.5 mM to 1.7 mM suggesting higher crosslinking density was achieved when H<sub>2</sub>O<sub>2</sub> concentration increased. However, further increase of H<sub>2</sub>O<sub>2</sub> concentrations resulted in a decline of  $G'$  which was likely due to the

deactivation of the HRP by an excess amount of H<sub>2</sub>O<sub>2</sub> [34]. Interestingly, the gel point of hydrogels with different H<sub>2</sub>O<sub>2</sub> concentrations remained at around 70 s, indicating that gelation rate was independent of H<sub>2</sub>O<sub>2</sub> concentration. In addition, the time required for  $G'$  to reach plateau increased with the increase of H<sub>2</sub>O<sub>2</sub> concentration. These results indicate that HRP was continuously oxidized by H<sub>2</sub>O<sub>2</sub> and reduced by HPA moieties, until all H<sub>2</sub>O<sub>2</sub> had been depleted in the process of Gtn-HPA hydrogel forming. Thus, it is considered that higher crosslinking density was achieved as a result of a higher amount of oxidized HPA, when the concentration of H<sub>2</sub>O<sub>2</sub> increased.

Fig. 3b shows the effects of HRP concentration on hydrogel formation while H<sub>2</sub>O<sub>2</sub> concentration was fixed at 1.7 mM.  $G'$  remains almost constant when the HRP concentration was above 0.02 units/ml. In contrast to the effect of H<sub>2</sub>O<sub>2</sub>, the gelation rate of Gtn-HPA hydrogels very much depended on the HRP concentration. Both the gel point and the time required for  $G'$  to reach plateau decreased concomitantly as HRP concentration increased. These results are in a good agreement with an earlier report of hyaluronic acid–tyramine hydrogel system using the same enzymatic oxidation reaction [12]. The mechanism of the independent tuning of gelation rate and stiffness of hydrogel has been explained in detail [13]. In this catalytic system, HRP catalyzed the crosslinking reaction with H<sub>2</sub>O<sub>2</sub> as the

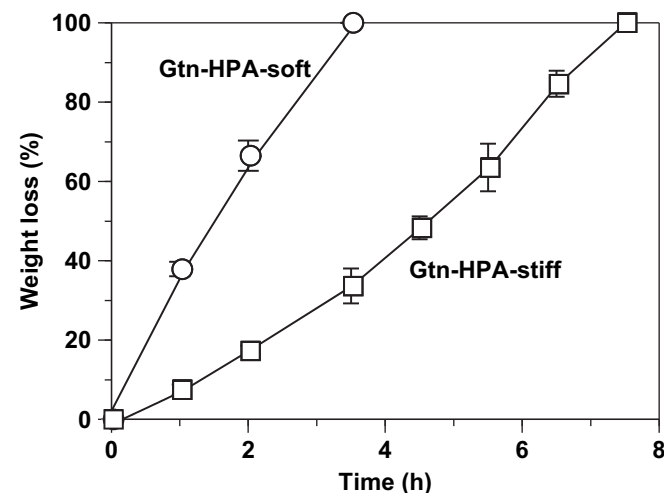


**Fig. 4.** Enzymatic degradation of Gtn-HPA hydrogels in the presence of 0.61 units/ml of type I collagenase at 37 °C. Results are shown as the average values ± standard deviation ( $n = 3$ ).

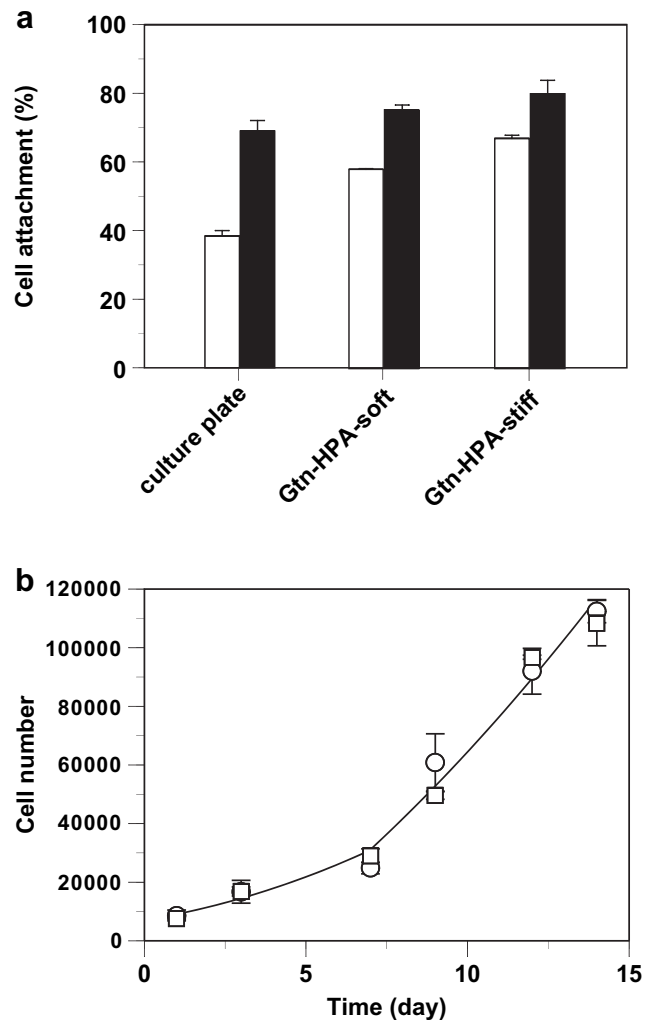


**Fig. 5.** (a) hMSC attachment on the surface of Gtn-HPA hydrogels after 1 h (open bar) and 6 h (filled bar) incubation. (b) 2D hMSC proliferation on Gtn-HPA-soft (○) and Gtn-HPA-stiff (□). Results are shown as the average values ± standard deviation ( $n = 4$ ).

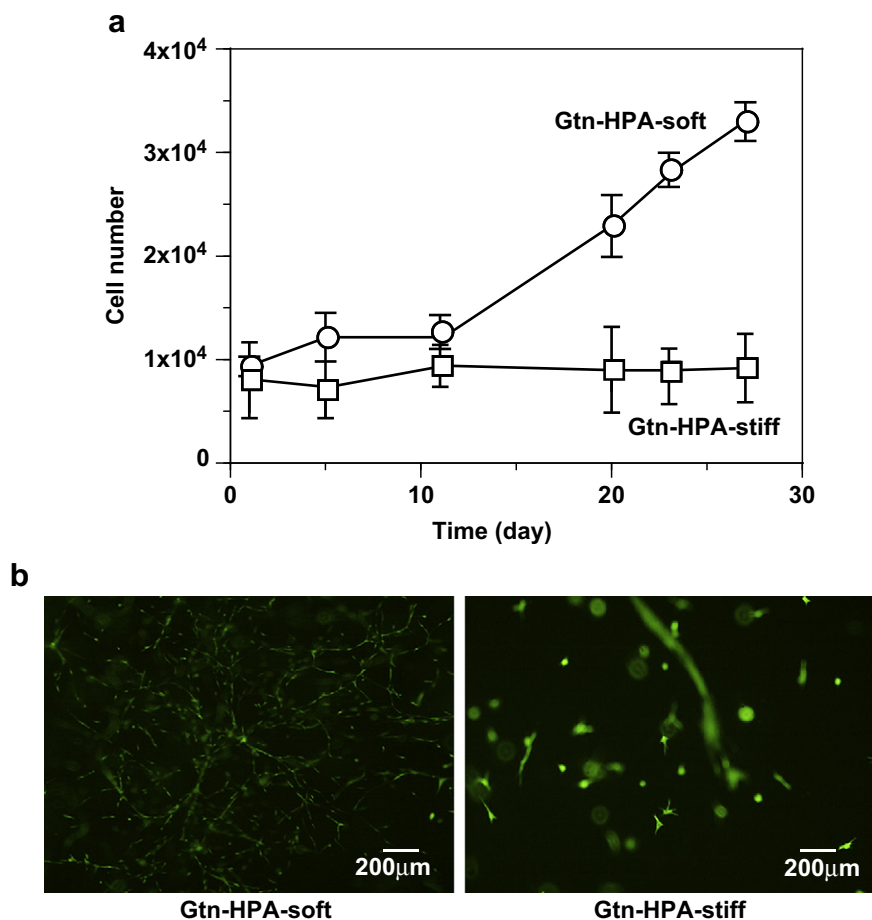


**Fig. 6.** (a) 3D hMSC proliferation in Gtn-HPA hydrogels. Results are shown as the average values  $\pm$  standard deviation ( $n = 6$ ). (b) Fluorescence images of hMSC cultured in Gtn-HPA hydrogels. The cells were stained by Calcein AM.

oxidant. After successive oxidations of two phenol molecules, HRP returned to its original state and re-entered the crosslinking cycle. Thus, the independent tuning achieved in Gtn-HPA hydrogels is considered to be due to the catalytic reaction of HRP and  $H_2O_2$ . The independent tuning of the Gtn-HPA hydrogel is expected to be useful as an injectable hydrogel system as such hydrogels can be formed at an efficient gelation rate with a wide range of stiffness. This unique independent tuning has not been seen in existing injectable hydrogel systems where the gelation rate is closely correlated to the stiffness.

Taking the ability of cell growth in hydrogels into account, the composition of hydrogel formation was optimized to provide the values of  $G'$  less than 1 KPa because poor cell proliferation was observed in the hydrogels of higher stiffness. The rheological properties of selected hydrogels for subsequent *in vitro* study were summarized in Table 1.  $G'$  of the hydrogels was significantly increased with increasing  $H_2O_2$  concentration; when 0.85 and 1.7 mM of  $H_2O_2$  concentration were used, the values of  $G'$  were  $281 \pm 19$  and  $841 \pm 45$  Pa, respectively. The hydrogels with different stiffness (281 and 841 Pa) are abbreviated respectively, as Gtn-HPA-soft and Gtn-HPA-stiff.

### 3.3. Degradation of hydrogels

Matrix metalloprotease (MMP) has been reported to degrade the extracellular matrix, leading to cell migration and growth in the body [35] and affect the degradability of proteolysis-sensitive hydrogels [36]. We assessed the enzymatic degradability of Gtn-HPA

hydrogels using type-1 collagenase, one of MMP family (Fig. 4). Gtn-HPA-soft degraded much faster than Gtn-HPA-stiff. This result suggests that the degradability can be well controlled by hydrogel stiffness and is expected to affect the proliferation rate of cells in hydrogels.

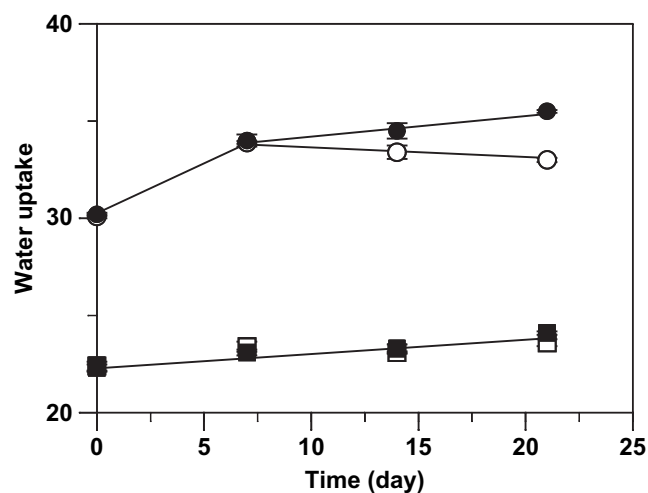


**Fig. 7.** Water uptake of Gtn-HPA-soft without cell ( $\circ$ ), Gtn-HPA-soft with cell ( $\bullet$ ), Gtn-HPA-stiff without cell ( $\square$ ) and Gtn-HPA-stiff with cell ( $\blacksquare$ ). Results are shown as the average values  $\pm$  standard deviation ( $n = 3$ ).

### 3.4. Cell attachment and proliferation on Gtn-HPA hydrogels

Prior to performing 3D cell culture in hydrogels, hMSCs were seeded on the surface of the hydrogels to evaluate cell attachment properties. Fig. 5a shows cell numbers of cells attached on culture plate, Gtn-HPA-soft and Gtn-HPA-stiff hydrogels expressed as a percentage with respect to the initial seeding number. The Gtn-HPA hydrogels provided an excellent support for cell attachment. The cell attachment on the Gtn-HPA hydrogels regardless their stiffness after 1 h incubation was significantly greater compared to the cell culture plate, and the hMSCs attached on the hydrogels continued to outnumber the ones on the culture plate during 6 h incubation. This good cell attachment behavior supported by the Gtn-HPA hydrogels is considered to be due to the positively charged residues and RGD peptide sequences of Gtn [37]. Also, the Gtn-HPA-stiff hydrogel achieved higher cell attachment after 1 h incubation compared to Gtn-HPA-soft. The cell attachment between hydrogels with different stiffness showed no significant difference after 6 h incubation. It has been reported that matrix stiffness affects morphology of hMSCs; the focal adhesion growth and elongation of the cell are promoted with increasing matrix stiffness ranging from 1 KPa to 34 KPa [8]. It is noteworthy that even though both hydrogels in our study are of  $G'$  less than 1 KPa, a significant difference in cell attachment was found for the first hour of incubation. Nevertheless, the difference was not significant after 6 h incubation.

Fig. 5b shows the proliferation of hMSCs on the surface of Gtn-HPA hydrogels with different stiffness. During 2 week culture of hMSCs on the hydrogel, cells continued to grow on both hydrogels without showing much difference in terms of the proliferation rate. As discussed above, there was no significant difference in cell numbers attached on the surface after 6 h between the two Gtn-HPA hydrogels. Hence, these results indicate that within the range of storage modulus (280–840 Pa), stiffness of these hydrogels has little effect on the proliferation rate of hMSCs cultured on the hydrogel surface.

### 3.5. 3D culture of hMSC in Gtn-HPA hydrogels

Given the evidence that Gtn-HPA hydrogel can be prepared under mild conditions, pairing with its biodegradability as well as cell adhesion property, the 3D culture of hMSCs inside Gtn-HPA hydrogels with different stiffness was explored. It was found that the cell proliferation was dependent on the stiffness of Gtn-HPA hydrogels (Fig. 6a). The rate of hMSCs proliferation increased with the decrease of the hydrogel stiffness, unlike the cell proliferation on the surface of the Gtn-HPA hydrogels discussed above. It suggested that this difference in the cell proliferation rate is attributed to the stiffness in a 3D environment, while the cells proliferated well on hydrogels regardless of their stiffness in a 2D context within the same stiffness range.

Fig. 6b represents the morphology of cells cultured in hydrogels after 2 weeks. The cells were stained by calcein acetoxymethyl ester (Calcein AM). hMSCs were allowed to grow inside the hydrogels. In the case of Gtn-HPA-soft, the hMSCs proliferated and formed inter-cell connections in the hydrogels with filopodia-rich morphology. However, the hMSCs in Gtn-HPA-stiff appeared to be much smaller due to the stiffer property resulting in a slower proliferation.

To understand the effects of hydrogel stiffness on cell proliferation in Gtn-HPA hydrogels, the water uptake of Gtn-HPA hydrogels with and without cells was measured (Fig. 7). For Gtn-HPA-soft without cells, the water uptake increased during the first week before reaching a plateau. In contrast, the water uptake in Gtn-HPA-soft with cells kept increasing and showed higher water uptake in comparison to Gtn-HPA-soft without cells. In the case of Gtn-HPA-stiff hydrogels, no significant difference in water uptake was found between the hydrogels with or without cells. The change of water uptake over time could be attributed to swelling of the hydrogel as a result of degradation or cross-linking efficiency. In a separate experiment, cross-linking efficiency for Gtn-HPA-soft and Gtn-HPA-stiff was determined. The dry weight of Gtn-HPA hydrogels was obtained by lyophilization was recorded after the hydrogels were soaked in water for 48 h. The dry weight without soaking in

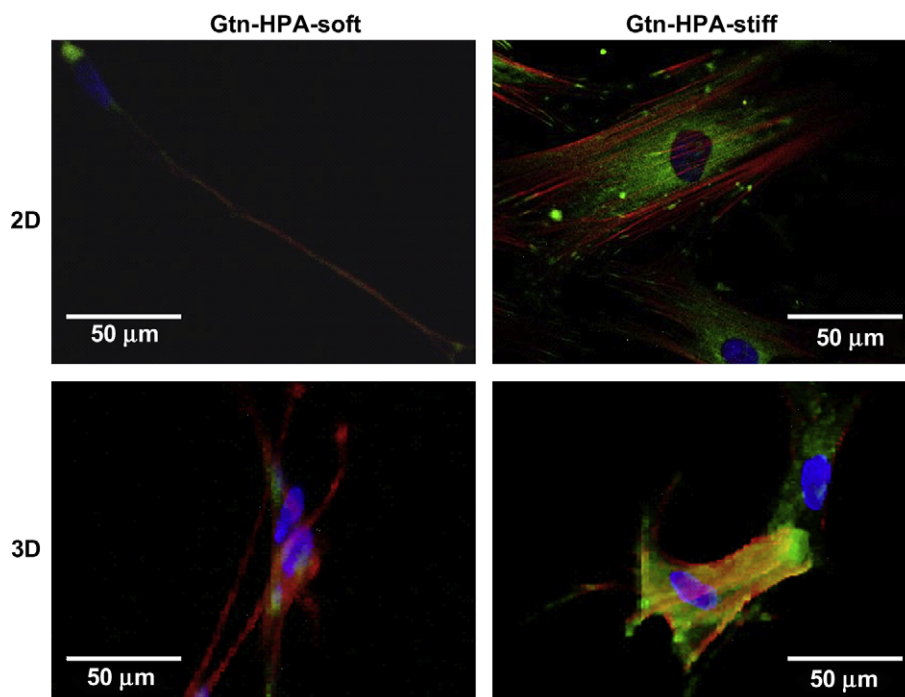
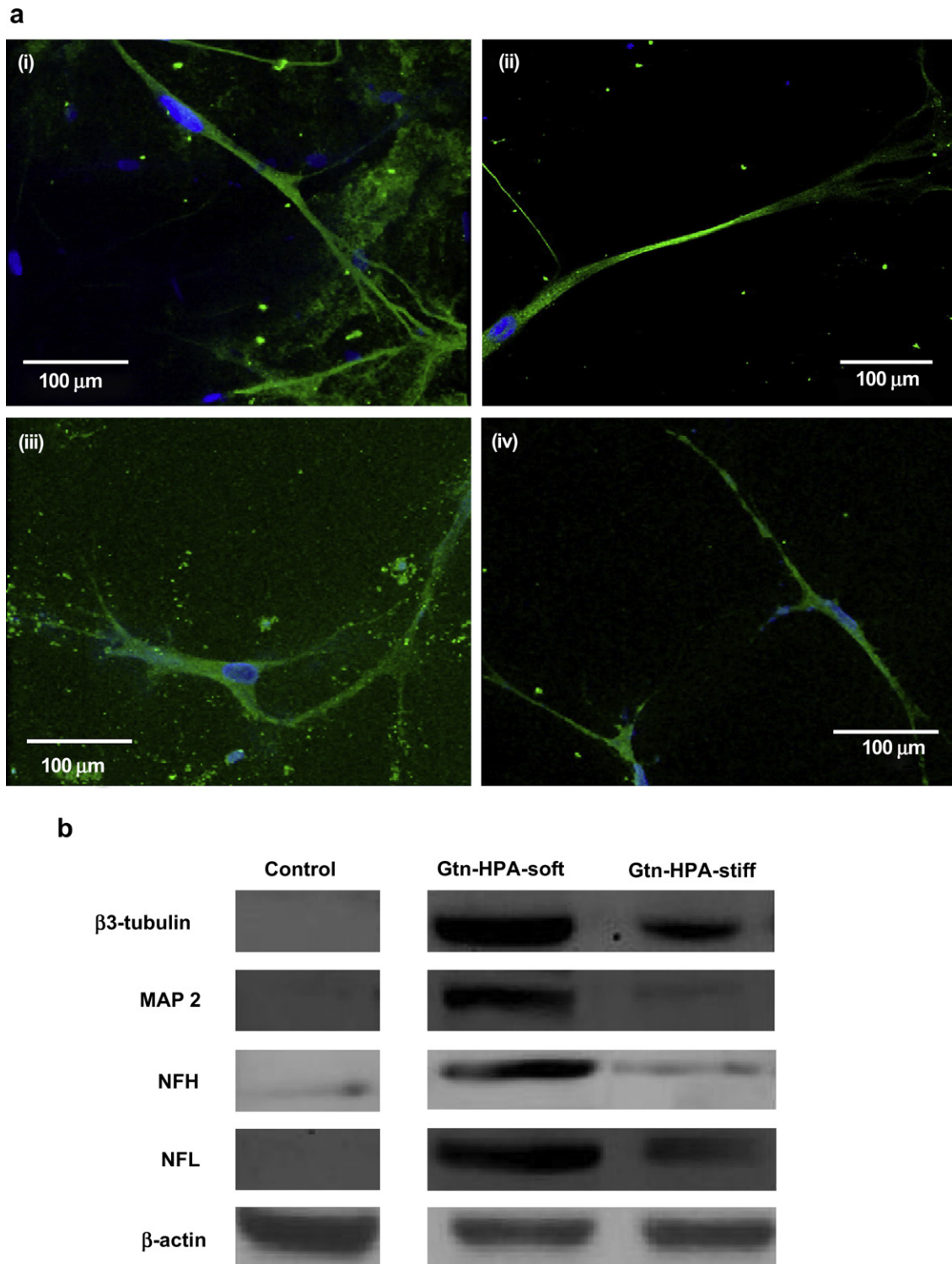


Fig. 8. Confocal fluorescence microscopy of focal adhesion and actin cytoskeleton in hMSCs cultured using Gtn-HPA hydrogels.

water was served as a control. It was found that 89% Gtn-HPA conjugate remained after soaking in the case of Gtn-HPA-soft. Whereas, there was 95% left for Gtn-HPA-stiff. Thus, it is suggested that for the Gtn-HPA-soft hydrogels, the increase of water uptake in the first week may be attributed to the leaching of uncrosslinked polymers. The continued increase in water uptake of the cell-encapsulated Gtn-HPA-soft for the subsequent two weeks is most

likely due to the degradation of the hydrogels. For the stiffer hydrogels, it is considered that the difference in the change of water uptake over time was much smaller compared to soft ones largely due to the higher stiffness resulting in a slower degradation. These results indicate that appropriate stiffness and degradability of the hydrogels play important roles in controlling 3D cell proliferation in hydrogels.



**Fig. 9.** (a) Immunofluorescence images of (i) β3-tubulin, (ii) NFL, (iii) MAP2, and (iv) NFH expressed in Gtn-HPA-soft hydrogels. (b) Western blotting of proteins expressed in Gtn-HPA hydrogels. Cells cultured on plastic culture plates were used as a control.

### 3.6. Focal adhesion study

To further study how the cells responded to the substrate stiffness, immunostaining of focal adhesion and actin cytoskeleton was performed. Fig. 8 shows the confocal fluorescence images of focal adhesion and actin cytoskeleton in hMSCs when the cells were cultured using Gtn–HPA hydrogels. These images reveal focal contacts in green using an anti-vinculin monoclonal antibody. Also, F-actin was detected in red and nuclear was shown in blue. In the 2D study, the cells appeared to be more spread out when they were cultured on a stiffer surface. Both focal contact and F-actin organization show a progressive trend, from diffused when in contact with soft hydrogels to a more organized arrangement in the case of stiffer ones. These results are in good agreement with the earlier reports on hMSC responding to matrix elasticity on collagen-coated polyacrylamide gels [8]. Despite the difference in the focal contact and F-actin arrangement between Gtn–HPA-soft and Gtn–HPA-stiff, it did not exert much influence on proliferation rate as shown above.

When the cells were cultured in a 3D environment, the focal contact and F-actin organization showed a similar trend compared to the observations from the 2D study. However, the proliferation rate of hMSCs in a 3D context was strongly affected by stiffness as discussed above. Thus, it is considered that the degradability of hydrogels is a dominant factor in controlling the cell proliferation, rather than the focal contact presentation and F-actin arrangement. These responses to substrate stiffness through focal contact presentation and F-actin arrangement may affect the differentiation of hMSCs, and are to be discussed in the following study.

### 3.7. hMSCs differentiation in Gtn–HPA hydrogels

To develop Gtn–HPA hydrogels for the neurogenesis of hMSCs in the 3D context, the cells were pre-treated with mitomycin C to inhibit proliferation and maintained inside the hydrogels with different stiffness in normal culture medium for 3 weeks. Mitomycin C was proven to have little impact on average cell shape and morphology [8]. Cells were then immunostained with neuron-specific antibodies: neurofilament light chain (NFL), late neuronal marker neurofilament heavy chain (NFH), mid/late neuronal marker microtubule associated protein 2 (MAP2) and neuron-specific marker  $\beta 3$  tubulin. Nuclei were counterstained with 4',6-diamidino-2-phenylindole (DAPI). In immunofluorescence images, cells in Gtn–HPA-soft revealed expression of these neuron-specific proteins (Fig. 9a). On the contrary, cells cultured on plastic culture plate over the same period of culture did not express the neuron-specific proteins (data not shown).

Western blotting was employed to quantify these expressed proteins. For cells harvested after 1 week of culture inside the Gtn–HPA hydrogels, only  $\beta 3$  tubulin was detectable in western blots (data not shown). The period of hMSCs culture in Gtn–HPA hydrogels was optimized to be 3 weeks to quantify protein markers of mid/late neurons (MAP2) and even mature neurons (NFL and NFH) (Fig. 9b). The expression of these protein markers was normalized to that of  $\beta$ -actin. The result confirmed that the hMSCs cultured inside the Gtn–HPA hydrogels for 3 weeks expressed protein markers for neuronal commitment, NFL, NFH, MAP2, and  $\beta 3$  tubulin, while cells cultured on plastic culture plate for the same period of time showed no neuronal protein marker expression. As mentioned, it has been reported that the differentiation of hMSCs on the surface of collagen-coated polyacrylamide gels [8]. Our results indicate that the neurogenesis of hMSCs in hydrogels can be also achieved if the appropriate stiffness of hydrogel is provided.

The neurogenesis was also strongly affected by hydrogel stiffness. Gtn–HPA-soft expressed much more neuronal protein markers compared to the Gtn–HPA-stiff. It has been suggested that

the focal contact and F-actin arrangement could affect the differentiation of hMSCs [8]. As discussed above, the hMSCs responded to substrate stiffness through the focal contact and F-actin arrangement. Thus, it is considered that neurogenesis in the Gtn–HPA hydrogels was largely affected by cell response in the focal adhesion due to stiffness. It is increasingly evident that cells do sense and respond to mechanical properties of the substrate in respect to a variety of cell functions, such as cell migration, spreading, growth and differentiation [38]. The result of cell proliferation and differentiation in Gtn–HPA hydrogels indicates that the design of a hydrogel scaffold with well-controlled mechanical properties is crucial in tissue engineering applications. Physical parameters are as important as biological and chemical parameters, in order to effectively repair, regenerate or engineer tissues.

## 4. Conclusion

An injectable and biodegradable Gtn–HPA hydrogel was formed by the oxidative coupling reaction of phenol moiety in the presence of  $H_2O_2$  and HRP. The stiffness of the hydrogel was well controlled by the  $H_2O_2$  concentration. The proliferation rate of 3D hMSC cultured in Gtn–HPA hydrogels was tuned by the hydrogel stiffness. hMSC neurogenesis in 3D was demonstrated using this hydrogel system, and the degree of neurogenesis was affected by the stiffness of hydrogel without the use of any biochemical signal, as confirmed by immunostaining and western blotting. This Gtn–HPA hydrogel system provides a simple and effective means to study cell functional responses in a 3D environment, given its *in situ* forming ability, excellent cell adhesion and tunable mechanical properties. With its biocompatibility and biodegradability, the Gtn–HPA hydrogel offers a promising system for regenerative applications of stem cells in tissue engineering and has the potential to further stem cell-based *in vivo* therapies. In the future, injectable Gtn–HPA hydrogels with tunable mechanical properties for 3D cell culture and differentiation would be an important strategic tool to treat neurological disorders or brain injuries.

## Acknowledgements

This work was supported by the Institute of Bioengineering and Nanotechnology (Biomedical Research Council, Agency for Science, Technology and Research, Singapore).

## Appendix

Figures with essential color discrimination. Figs. 1, 6, 8 and 9 in this article are difficult to interpret in black and white. The full color images can be found in the on-line version, at doi:10.1016/j.biomaterials.2009.10.042.

## References

- [1] Bianco P, Robey PG. Stem cells in tissue engineering. *Nature* 2001;414(6859):118–21.
- [2] Chai C, Leong KW. Biomaterials approach to expand and direct differentiation of stem cells. *Mol Ther* 2007;15(3):467–80.
- [3] Hwang NS, Varghese S, Elisseeff J. Controlled differentiation of stem cells. *Adv Drug Deliv Rev* 2008;60(2):199–214.
- [4] Bianco P, Riminucci M, Gronthos S, Robey PG. Bone marrow stromal stem cells: nature, biology, and potential applications. *Stem Cells* 2001;19(3):180–92.
- [5] Barberi T, Bradbury M, Dincer Z, Panagiotakos G, Socci ND, Studer L. Derivation of engraftable skeletal myoblasts from human embryonic stem cells. *Nat Med* 2007;13(5):642–8.
- [6] Discher DE, Janmey P, Wang YL. Tissue cells feel and respond to the stiffness of their substrate. *Science* 2005;310(5751):1139–43.
- [7] Yim EK, Pang SW, Leong KW. Synthetic nanostructures inducing differentiation of human mesenchymal stem cells into neuronal lineage. *Exp Cell Res* 2007;313(9):1820–9.

- [8] Engler AJ, Sen S, Sweeney HL, Discher DE. Matrix elasticity directs stem cell lineage specification. *Cell* 2006;126(4):677–89.
- [9] Abdallah BM, Kassem M. Human mesenchymal stem cells: from basic biology to clinical applications. *Gene Ther* 2008;15(2):109–16.
- [10] Alsberg E, Anderson KW, Albeiruti A, Rowley JA, Mooney DJ. Engineering growing tissues. *Proc Natl Acad Sci U S A* 2002;99(19):12025–30.
- [11] Gupta D, Tator CH, Shoichet MS. Fast-gelling injectable blend of hyaluronan and methylcellulose for intrathecal, localized delivery to the injured spinal cord. *Biomaterials* 2006;27(11):2370–9.
- [12] Lee F, Chung JE, Kurisawa M. An injectable enzymatically crosslinked hyaluronic acid-tyramine hydrogel system with independent tuning of mechanical strength and gelation rate. *Soft Matter* 2008;4:880–7.
- [13] Lee F, Chung JE, Kurisawa M. An injectable hyaluronic acid-tyramine hydrogel system for protein delivery. *J Control Release* 2009;134(3):186–93.
- [14] Kurisawa M, Chung JE, Yang YY, Gao SJ, Uyama H. Injectable biodegradable hydrogels composed of hyaluronic acid-tyramine conjugates for drug delivery and tissue engineering. *Chem Commun (Camb)* 2005;34:4312–4.
- [15] Burdick JA, Ward M, Liang E, Young MJ, Langer R. Stimulation of neurite outgrowth by neurotrophins delivered from degradable hydrogels. *Biomaterials* 2006;27(3):452–9.
- [16] Zhong Y, Bellamkonda RV. Biomaterials for the central nervous system. *J R Soc Interface* 2008;5(26):957–75.
- [17] Comolli N, Neuhofer B, Fischer I, Lowman A. In vitro analysis of PNIPAAm-PEG, a novel, injectable scaffold for spinal cord repair. *Acta Biomater* 2009;5(4):1046–55.
- [18] Piantino J, Burdick JA, Goldberg D, Langer R, Benowitz LI. An injectable, biodegradable hydrogel for trophic factor delivery enhances axonal rewiring and improves performance after spinal cord injury. *Exp Neurol* 2006;201(2):359–67.
- [19] Horn EM, Beaumont M, Shu XZ, Harvey A, Prestwich GD, Horn KM, et al. Influence of cross-linked hyaluronic acid hydrogels on neurite outgrowth and recovery from spinal cord injury. *J Neurosurg Spine* 2007;6(2):133–40.
- [20] Hou S, Xu Q, Tian W, Cui F, Cai Q, Ma J, et al. The repair of brain lesion by implantation of hyaluronic acid hydrogels modified with laminin. *J Neurosci Methods* 2005;148(1):60–70.
- [21] Tian WM, Hou SP, Ma J, Zhang CL, Xu QY, Lee IS, et al. Hyaluronic acid-poly-D-lysine-based three-dimensional hydrogel for traumatic brain injury. *Tissue Eng* 2005;11(3–4):513–25.
- [22] Woerly S, Marchand R, Lavallec C. Intracerebral implantation of synthetic polymer/biopolymer matrix: a new perspective for brain repair. *Biomaterials* 1990;11(2):97–107.
- [23] Martin BC, Minner EJ, Wiseman SL, Klank RL, Gilbert RJ. Agarose and methylcellulose hydrogel blends for nerve regeneration applications. *J Neural Eng* 2008;5(2):221–31.
- [24] Brannvall K, Bergman K, Wallenquist U, Svahn S, Bowden T, Hilborn J, et al. Enhanced neuronal differentiation in a three-dimensional collagen-hyaluronan matrix. *J Neurosci Res* 2007;85(10):2138–46.
- [25] Willerth SM, Arendas KJ, Gottlieb DI, Sakiyama-Elbert SE. Optimization of fibrin scaffolds for differentiation of murine embryonic stem cells into neural lineage cells. *Biomaterials* 2006;27(36):5990–6003.
- [26] Thonhoff JR, Lou DI, Jordan PM, Zhao X, Wu P. Compatibility of human fetal neural stem cells with hydrogel biomaterials in vitro. *Brain Res* 2008;1187:42–51.
- [27] Wu S, Suzuki Y, Kitada M, Kitaura M, Kataoka K, Takahashi J, et al. Migration, integration, and differentiation of hippocampus-derived neurosphere cells after transplantation into injured rat spinal cord. *Neurosci Lett* 2001;312(3):173–6.
- [28] Krabbe C, Zimmer J, Meyer M. Neural transdifferentiation of mesenchymal stem cells—a critical review. *APMIS* 2005;113(11–12):831–44.
- [29] Hu M, Kurisawa M, Deng R, Teo CM, Schumacher A, Thong YX, et al. Cell immobilization in gelatin-hydroxyphenylpropionic acid hydrogel fibers. *Biomaterials* 2009;30(21):3523–31.
- [30] Snyder SL, Sobocinski PZ. An improved 2,4,6-trinitrobenzenesulfonic acid method for the determination of amines. *Anal Biochem* 1975;64(1):284–8.
- [31] Lee KY, Mooney DJ. Hydrogels for tissue engineering. *Chem Rev* 2001;101(7):1869–79.
- [32] Sakai S, Hirose K, Taguchi K, Ogushi Y, Kawakami K. An injectable, in situ enzymatically gellable, gelatin derivative for drug delivery and tissue engineering. *Biomaterials* 2009;30(20):3371–7.
- [33] Oudgenoeg G, Hilhorst R, Piersma SR, Boeriu CG, Gruppen H, Hessing M, et al. Peroxidase-mediated cross-linking of a tyrosine-containing peptide with ferulic acid. *J Agric Food Chem* 2001;49(5):2503–10.
- [34] Schmidt A, Schumacher JT, Reichelt J, Hecht HJ, Bilitewski U. Mechanistic and molecular investigations on stabilization of horseradish peroxidase C. *Anal Chem* 2002;74(13):3037–45.
- [35] Basbaum CB, Werb Z. Focalized proteolysis: spatial and temporal regulation of extracellular matrix degradation at the cell surface. *Curr Opin Cell Biol* 1996;8(5):731–8.
- [36] Lutolf MP, Lauer-Fields JL, Schmoekel HG, Metters AT, Weber FE, Fields GB, et al. Synthetic matrix metalloproteinase-sensitive hydrogels for the conduction of tissue regeneration: engineering cell-invasion characteristics. *Proc Natl Acad Sci U S A* 2003;100(9):5413–8.
- [37] Lee SB, Jeon HW, Lee YW, Lee YM, Song KW, Park MH, et al. Bio-artificial skin composed of gelatin and (1 → 3), (1 → 6)-beta-D-glucan. *Biomaterials* 2003;24(14):2503–11.
- [38] Drury JL, Mooney DJ. Hydrogels for tissue engineering: scaffold design variables and applications. *Biomaterials* 2003;24(24):4337–51.